Poly(lactic-co-glycolic) acid nanoparticles as a delivery system for fish oil in wound healing

Tomáš Komprda[1], Vendula Popelková[1], Ludmila Košarišťanová[2], Veronika Šmídová[2]

Mendel University in Brno, Faculty of AgriSciences, [1]Department of Food Technology, [2]Department of Chemistry and Biochemistry, Brno, Czech Republic

Received November 3, 2021
Accepted June 14, 2022

Abstract

The objective of the study was to design, synthetize and characterize poly(lactic-co-glycolic) acid (PLGA) nanoparticles (NPs) with entrapped fish oil (FO) for possible application in a cutaneous wound healing. Morphology of NPs was evaluated by transmission electron microscopy. Antimicrobial characteristics were tested using the disk diffusion method and plate count method, and cytotoxicity was evaluated by the MTT assay. Fish oil (y) was released from PLGA NPs within the time interval (x) of 96 h according to equation y = 6.2 + 0.914x. PLGA-FO NPs did not affect growth of *Staphylococcus aureus* or methicillin-resistant *S. aureus* (MRSA) strains. No cytotoxic effect of the tested NPs on the keratinocyte cell line was observed for concentration of 1 µg/ml. PLGA-FO NPs represent an interesting alternative for wound healing due to an excellent biocompatibility and unique release profile of FO, despite their lack of antimicrobial efficiency.

Polyunsaturated fatty acids n-3, drug encapsulation, drug release profile, ζ-potential, Staphylococcus aureus, cell viability

Poly(lactic-co-glycolic) acid (PLGA) can carry antibiotics or/and anti-inflammatory and antioxidant drugs. As biodegradable polymer, it is suitable for the production of nanoparticles (NPs) of a clinical interest because it protects loaded drugs from biological degradation and due to enhanced stability and sustained release, it allows a reduction of the administrated dose (Berthet et al. 2017). Due to the excellent biocompatibility and adjustable mechanical properties, PLGA is widely used as a drug carrier that improves drug delivery and absorption by oral or parenteral administration (Kemme and Heinzel-Wieland 2018).

In terms of substances that are potentially usable as components of the NPs-based drug-delivery carriers, one interesting possibility is fish oil (FO) due to its anti-inflammatory and anti-oxidant properties (Giustina et al. 2020). Fish oil entrapment in NPs is still rather uncommon, but it was recently used e.g. by Rakotoarisoa et al. (2019) in curcumin- and FO-loaded spongosome and cubosome NPs. The positive effects of the FO key components, long-chain polyunsaturated fatty acids n-3 (LC-PUFA n-3: eicosapentaenoic acid, EPA and docosahexaenoic acid, DHA) on human health are wide-ranging and include skin wound healing (Komprda 2018). Regarding the four main stages of skin repair (haemostasis, inflammation, proliferation and remodelling), LC-PUFA n-3 anti-inflammatory effects are highlighted in terms of competition with arachidonic acid in eicosanoid synthesis and of a modulation of signalling pathways mediated by transcription factors nuclear factor kappa B, peroxisome proliferator-activated receptors, and sterol response element-binding proteins (Komprda 2012). We have recently applied dietary FO in the rat model of cutaneous wound healing (Komprda et al. 2020). Arantes et al. (2016) reported accelerated wound healing using DHA in a topical treatment of a cutaneous excision.

The objective of the present study was to design and synthetize biodegradable, stable and biocompatible polymeric PLGA NPs with entrapped fish oil, to characterize them from the

Address for correspondence:
Tomáš Komprda
Department of Food Technology
Mendel University in Brno
Zemědělská 1, 613 00 Brno, Czech Republic
E-mail: komprda@mendelu.cz
http://actavet.vfu.cz/

viewpoint of the size distribution, polydispersity index, zeta potential, loading capacity and the release profile of the entrapped FO and to test their cytotoxicity and antimicrobial activities with an intention to assess their suitability for cutaneous wound healing.

Materials and Methods

Synthesis of the nanoparticles

Following chemicals were used for the production of NPs: dichloromethane (DCM, anhydrous: 99.8%; Sigma-Aldrich, St. Louis, MO, USA); fish oil (FO; cod liver oil; Sigma-Aldrich); poly(lactic-co-glycolic) acid (PLGA; Mw 38,000–54,000 g/mol; lactide:glycolide ratio of 50:50; Sigma-Aldrich); hexane (95%; JT Baker Chemical Co., Phillipsburg, NJ); polyvinyl alcohol (PVA, 98–99%, hydrolysed, Mw 31,000–50,000 g/mol; Sigma-Aldrich); trehalose dihydrate, 99.0%, Mw 378,33 g/mol; Sigma-Aldrich); nano-pure water (Nanopure Diamond; USA); 0.2 µm Barnsted D3750 Hollow Fiber Filter (Barnsted International, Dubuque, IA, USA); ethyl acetate (EMD Chemicals Inc., Gibbstown, NJ, USA); acetonitrile (EMD Chemicals).

Nanoparticles were synthesized by the emulsion evaporation. In the case of NPs with entrapped FO (PLGA-FO-PVA NPs), the organic phase was prepared by mixing 440 mg of PLGA, 10 ml of DCM and 200 mg of fish oil. The aqueous phase of 2% PVA was prepared by stirring (400 rpm) at 60 °C. The organic phase was added to the aqueous phase drop-wise by stirring at 220 rpm and the formed emulsion was microfluidized 4 × at 30,000 psi using a microfluidizer M 110P (Microfluidics, MA, USA). The solvent was then evaporated under vacuum using a rotoevaporator (R-124, Rotovap, Buchi Inc., New Castle, DE, USA) for 45 min (800 mm Hg methylene chloride). Nanoparticles were then dialyzed for two days (25 °C) to remove excess PVA using 300 kDa Spectra/POR CE membrane (Spectrum Rancho, CA, USA). Consequently, the samples were mixed (1:1, w/w) with 100 mg of trehalose, frozen for 30 min in freezer and then freeze-dried for two days (2.5-plus freezone; Labconco Corporation, MO, USA). The NP powder was stored in the dark, refrigerated conditions (under −20 °C) until further analysis. Empty NPs (PLGA-PVA NPs) were prepared by the same procedure as in the case of PLGA-FO-PVA NPs, only without fish oil.

Physical characteristics of nanoparticles

The morphology of NPs was studied by transmission electron microscopy (TEM). The lyophilized NPs sample was re-suspended in water (in a 20 ml vial) to a concentration of 5 $mg \cdot ml^{-1}$ and sonicated in a water bath for 5 min. One droplet (3 µl) of the sample was placed on the discharged 300-mesh carbon film grid (TEM-CF300-cu; Sigma-Aldrich). After 2 min, excess liquid was removed by a filter paper, the grid was stained with 2% of uranyl acetate as a contrast agent and the sample was imaged using a JEOL JEM-1400 apparatus (JEOL USA Inc., Peabody, MA, USA).

The size distribution (polydispersity index, PI) and ζ-potential of the NPs were measured by the light dynamic scattering (DLS) using a Malvern Zetasizer Nano ZS (Malvern Instruments Ltd., Worcestershire, U.K.) after dissolving the lyophilized samples in water at a concentration of 0.25 mg/ml and placing them into disposable capillary cell (Malvern Panalytical Inc., Westborough, MA, USA).

The evaluation of the release profile, including loading capacity (LC; dimensionless number) and entrapment efficiency (EE; in %) of FO from NPs was performed as follows. The freeze-dried NPs sample was resuspended in deionized water to a concentration of 15 $mg \cdot ml^{-1}$ under sonication for 5 min (Branson 3510, USA). Fifteen ml of the suspension was then placed into a dialysis tube equipped with Spectra/por Dialysis membrane (Mw 300 kD; Fisher Scientific, USA) and shaken at 37 °C and 95 rpm in an incubator shaker C25 KC (New Brunswick Scientific Inc., Edison, NJ, USA). A volume of 200 µl of the suspension was taken out from the dialysis tube at each time point of 0, 2, 4, 6, 24, 48, 72, 96 h, and 1.8 ml of hexane was added. Then the sample was shaken in a vortex for 5 min and consequently centrifuged at 44,800 *g* for 20 min at 10 °C (Allegra 64R centrifuge, Beckman Coulter, Inc., CA, USA). Supernatant was removed and absorbance was measured by a UV/Vis spectrophotometer (Genesis 6, ThermoFisher Scientific, Waltham, MA, USA) at 320 nm. The measurements were performed in triplicate. The concentration of the respective active substance was determined based on a standard curve measured under the same conditions.

The LC and EE values were calculated as follows:

LC = [amount of the active substance in the NPs (µg)]/ [total amount of the NPs (mg)];

EE (%) = [amount of the active substance in the system on start (µg) – free active substance]/ [amount of the active substance in the system on start (µg)] × 100.

Microbiological evaluation

For the microbiological evaluation, the tested samples of NPs were dissolved in MilliQ water and sonicated for 5 min (40 KHz).

Cultivation of the tested bacterial strains

Staphylococcus aureus (CCM 4223) and MRSA (CCM 7110) were obtained from the Czech Collection of Microorganisms (Brno, Czech Republic). The bacterial strains were cultured on 5% Columbia blood agar (LMS, Czech Republic) at 37 °C overnight.

Disk diffusion method

Bacterial cultures were diluted in saline to reach a cell density of 0.5 McFarland turbidity standard. The bacterial suspension was spread by a sterile cotton swab on a Petri dish with Muller Hinton agar (Oxoid, UK). Cellulose discs (Oxoid, UK) with 10 µl of the dissolved sample of PLGA-FO-PVA NPs (1 mg·ml^{-1}), PLGA-empty-PVA (0.5 mg·ml^{-1}) and PLGA-empty-PVA (1 mg·ml^{-1}), and control antibiotics (penicillin for *S. aureus*; vancomycin for MRSA), were applied on prepared Petri dishes with a particular bacterial strain. A diameter of the inhibition zones was measured after 18 h of incubation at 37 °C.

Growth curve

The bacterial strains (*S. aureus*; MRSA) were diluted in Mueller Hinton broth (2 × concentrated; Oxoid, UK) to 0.5 McFarland units and then diluted 100 × to reach a cell density of 1–2 × 10^6 CFU·ml^{-1}. The diluted strains of bacteria were placed in 100-well honeycomb microplates and PLGA-FO-PVA NPs and PLGA-empty-PVA NPs, respectively, dissolved in MilliQ water were added, thus creating a concentration of 0.5 mg·ml^{-1}. Then the half-dilution concentration series was performed for every tested sample. The growth curve of bacteria was measured by Bioscreen C MBR (Oy Growth Curves Ab Ltd., Finland). The absorbance reads at 620 nm were monitored at time zero and then at 30 min intervals for 24 h at 37 °C.

Cytotoxicity testing

Spontaneously transformed aneuploid immortal keratinocyte cell line from adult human skin (HaCaT) was cultured in RPMI-1640 medium with 10% foetal bovine serum, supplemented with penicillin (100 U·ml^{-1}) and streptomycin (0.1 mg·ml^{-1}). The treatment was initiated after the cells reached ~ 60–80% confluence. Cells were then harvested, washed 4 × with PBS (pH 7.4) and counted using Countess IIFL Automated Cell Counter (Life Technologies, Carlsbad, CA, USA).

Cell viability was estimated using the MTT assay. Briefly, the suspension of 5 000 cells in 50 µl medium was added to each well of microtitre plates (E-plates 96), followed by incubation for 24 h at 37 °C with 5% CO_2 to ensure cell growth. Fifty µl of medium containing PLGA–FO–PVA or PLGA–empty–PVA were added to the cells. Treated cells were incubated for 24 h. Further, 10 µl of 3–(4,5–dimethylthiazol–2–yl)–2,5–diphenyltetrazolium bromide (MTT [5 mg·ml^{-1} in PBS]) were added to the cells and the mixture was incubated for 4 h at 37 °C. MTT-containing medium was replaced by 100 µl of 99.9% dimethyl sulphoxide to dissolve MTT-formazan crystals and, after 5 min incubation, absorbance of the samples was determined at 570 nm (VersaMax microplate reader, Molecular Devices, Sunnyvale, CA, USA).

Statistical evaluation

The differences between the tested samples were statistically evaluated by one-way ANOVA with *post hoc* Tukey's test using the Statistica 12 package (StatSoft, Tulsa, OK, USA). A value of $P < 0.05$ was considered significant.

Results

Morphology and zeta potential of NPs

The size and shape of the PLGA NPs (empty or with entrapped fish oil) is apparent from Fig. 1 (Plate XV). The lightened layer on the surface of the NPs is formed by a surfactant polyvinyl alcohol (PVA).

As shown in Table 1, the size of NPs was in the range between 190 and 233 nm. Sizes of the particles were heterogeneous, as indicated by the relatively high values of the polydispersity index. Both tested types of NPs were negatively charged, the loaded NPs substantially more (higher zeta potential) than the empty ones.

Table 1. Selected characteristics of poly(lactic-co-glycolic) acid (PLGA)-polyvinyl alcohol (PVA) nanoparticles (NPs) either empty or with entrapped fish oil (FO).

Type of NPs	Mean size (diameter in nm)	Zeta potential (mV)	Polydispersity index (A.U.)
PLGA-PVA (empty)	190.7 ± 1.9	–4.95 ± 3.5	0.218 ± 0.018
PLGA-FO-PVA	233.3 ± 23.3	–68.10 ± 1.0	0.351 ± 0.016

Entrapment efficiency, loading capacity, and fish oil release from NPs

Fish oil entrapment efficiency was 22.5% and the FO loading capacity to the PLGA NPs was 22.4 µg FO/mg powder. As depicted in Fig. 2, the time dependence of the release of the entrapped FO from PLGA-PVA NPs was linear.

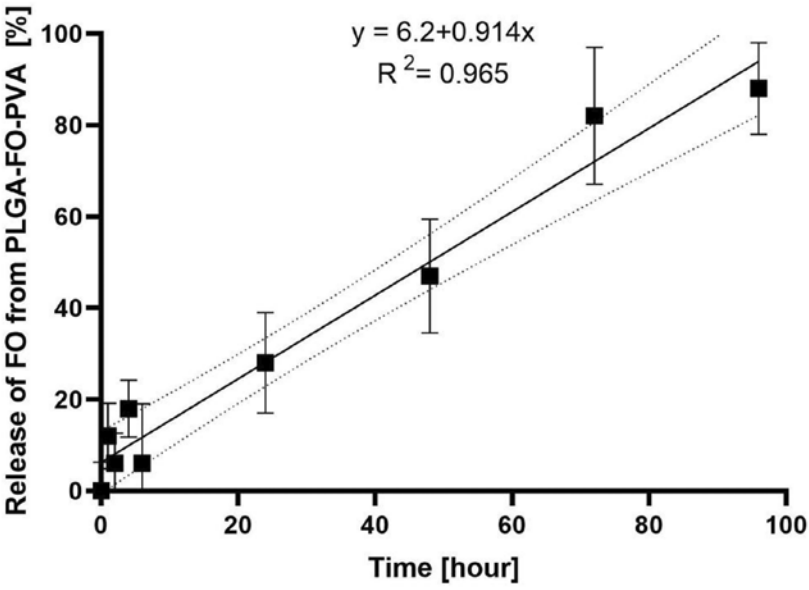

Fig. 2. Release profle of fsh oil (FO) from poly(lactic-co-glycolic) acid (PLGA)-polyvinyl alcohol (PVA) nanoparticles

Antimicrobial efficiency

Antimicrobial e f ciency of the empty and loaded PLGA NPs was tested on *S. aureus* and MRSA strains. Neither PLGA-empty-PVA NPs nor PLGA-FO-PVA NPs a f ected the growth curve of any tested bacterial strain (data not shown). Similarly, neither of the tested NPs (empty; FO-loaded) showed inhibition activity against the selected bacterial strains evaluated by the disk di f usion method (Plate XV, Fig. 3).

Cytotoxicity testing

The *in vitro* potential cytotoxic activity of empty PLGA-PVA nanoparticles and PLGA-PVA nanoparticles with entrapped fsh oil against keratinocyte cell line HaCaT was quanti f ed by the MTT assay. Percentage of the viable cells versus concentration of the empty or loaded NPs sample is shown in Fig. 4. Both types of the tested PLGA-PVA nanoparticles at the concentration of 0.5 mg·ml^{-1} increased the keratinocyte cell death rate above 50%; the keratinocyte viability ranged between 60–65% when the concentration of 0.25 mg·ml^{-1} of the tested samples was applied.

The most important fnding as shown in Fig. 4 was the substantially lower cell mortality rate ($P < 0.05$) of PLGA-FO-PVA NPs in comparison with the empty NPs at all NP concentrations below 60 µg·ml^{-1}.

Discussion

Morphology, ζ-potential, release profile

The average size of the PLGA NPs used in the present study (190–233 nm; Table 1) is comparable with the values reported for PLGA nanoparticles loaded with di f erent

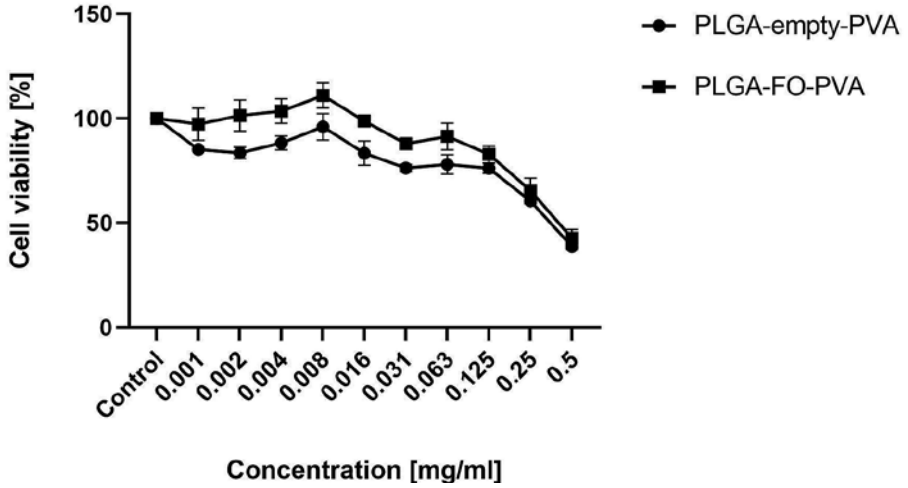

Fig. 4. Cytotoxic effect of increasing concentrations of poly(lactic-co-glycolic) acid (PLGA)-polyvinyl alcohol (PVA) nanoparticles (NPs) either empty (PLGA-empty-PVA) or with entrapped fish oil (PLGA–FO–PVA) on HaCaT cells analysed by the MTT assay (control – medium alone)

kinds of antibiotics (Hasan et al. 2019; Cheng et al. 2021). However, the polydispersity index of the PLGA NPs was much lower in the quoted experiments (0.045 and 0.10–0.15, respectively) in comparison with the present study (0.22–0.35), where PLGA NPs were more heterogeneous.

Surface of the PLGA NPs used in the present study was negatively charged (likely due to the presence of the carboxyl groups in the PLGA NPs); ζ-potential of the FO-loaded NPs was 13-times higher in comparison with unloaded particles. Similarly, Liu et al. (2021) reported also a relatively high ζ-potential of the PLGA NPs loaded with DHA (FO component).

The main release mechanism from PLGA NPs is diffusion- and degradation-controlled (Son et al. 2017). In any case, the release profile of FO from PLGA NPs (linear time dependence; Fig. 2) was conspicuously different from the data regarding antibiotics (Hasan et al. 2019; Petinelli et al. 2020; Cheng et al. 2021).

No data concerning FO entrapment efficiency in NPs are found in the available literature. The results of the present study (entrapment efficiency of 22.5%) can only be compared with the data reported by Yang and Ciftci (2020), who reported FO loading efficiency to be 92.3% in microparticles (average particle size of 6.9 μm) prepared by atomization of the CO_2-expanded lipid mixture.

The PLGA NPs tested in the present study were synthesized using the organic solvent dichloromethane (DCM) which is a suspected carcinogen and mutagen, and therefore needs to be removed from the NPs. The International Conference on Harmonization of Technical Requirements for Registration of Pharmaceuticals for Human Use established the limit of residual DCM of less than 600 ppm (Han et al. 2012). Because the NPs tested in the present study were intended for medical use, the question of residual DCM should be addressed. The steps of the PLGA NPs synthesis included solvent evaporation, two-day dialysis and two-day freeze-drying (see the Materials and Methods section above). Low solubility in water and low boiling point allows a convenient removal of DCM by evaporation (Meng et al. 2003). We did not measure residual DCM in the NPs in our study, but we can accept the results of Han et al. (2012) who reported a mean residual

DCM content of 377 ppm (i.e. safely below the above-mentioned limit of 600 ppm) using "typical synthesis methods", which was similar to our procedure, but even with shorter dialysis and freeze-drying steps.

Microbiological markers

A lack of anti-microbial activity of PLGA-FO NPs found out in the present study does not agree with the results of Hashim et al. (2019), who reported significant antimicrobial activity of FO encapsulated in polymeric microbeads. Moreover, Kendall et al. (2017) consider PUFA n-3 useful in the treatment of skin injuries due to their healing and anti-inflammatory effects.

Cytotoxicity

According to Cheng et al. (2021), using PLGA NPs as a drug delivery system may decrease toxicity effects due to the slow release of the drug. However, unloaded poly(hydroxybutyrate-co-hydroxyvalerate) microparticles decreased proliferation of embryonic fibroblasts in comparison with control in a study by Pettinelli et al. (2020). In the present experiment, FO-loaded PLGA NPs significantly ($P < 0.05$) increased keratinocyte viability compared to the empty PLGA NPs. Rakotoarisoa et al. (2019) reported no significant human neuroblastoma cell death using FO/curcumin-loaded spongosome/cubosome NPs in MTT viability assay.

In conclusion, as far as wound healing is concerned, either drug-loaded NPs or fish oil alone are broadly used. However, entrapment of fish oil into the PLGA NPs is original for this study. PLGA-FO NPs have excellent biocompatibility, and a sustained linear release of FO during 96 h is advantageous for the given purpose. So, despite a lack of antimicrobial efficiency, the FO-loaded NPs deserve further study, including a possible application on the cutaneous wound healing.

Acknowledgement

The experiment was supported by the Internal Grant Agency of the Faculty of AgriSciences of the Mendel University in Brno, project No. AF-IGA2019-TP006.

References

Arantes EL, Dragano N, Ramalho A, Vitorino D, de Souza GF, Lima MH, Velloso MA, Araújo EP 2016: Topical docosahexaenoic acid (DHA) accelerates skin wound healing in rats and activates GPR120. Biol Res Nutr **18** 411-419

Berthet M, Gauthier Y, Lacroix C, Verrier B, Monge C 2017: Nanoparticle-based dressing: The future of wound treatment? Trends Biotech **35**: 770-784

ChengY-H, Chang YF, Ko Y-C, Jui-ling Liu C 2021: Development of a dual delivery of levofoxacin and prednisolone acetate via PLGA nanoparticles/thermosensitive chitosan-based hydrogel for postoperative management: An *in-vitro* and *ex-vivo* study. Int J Biol Macromol **180**: 365-374

Giustina AD, de Souza Goldim MP, Gainski Danielski L, Garbossa L, Oliveira Junior AN, Cidreira T, Denico T, Bonfante S, da Rosa N, Fortunato JJ, Palandi J, Hofmann de Oliveira B, Fernandes Martins D, Bobinski F, Garcez M, Bellettini-Santos T, Budni J, Colpo G, Scaini G, Giridharan VV, Barichello T, Petronilho F 2020: Lipoic acid and fish oil combination potentiates neuroinflammation and oxidative stress regulation and prevents cognitive decline of rats after sepsis. Mol Neurobiol **57**: 4451-4466

Han E-J, Chung A-H, Oh I-J 2012: Analysis of residual solvents in poly(lactide-co-glycolide) nanoparticles. J Pharm Investig **42**: 251-256

Hasan N, Cao J, Lee J, Hlaing SP, Oshi MA, Naeem M, Ki M-H, Lee BL, Jung Y, Yoo J-W 2019: Bacteria-targeted clindamycin loaded polymeric nanoparticles: Effect of surface charge on nanoparticle adhesion to MRSA, antibacterial activity, and wound healing. Pharmaceutics **11**: 236

Hashim AF, Hamed SF, Abdel Hamid HA, Abd-Elsalam KA, Golonka I, Musiał W, El-Sherbiny IL 2019: Antioxidant and antibacterial activities of omega-3 rich oils/curcumin nanoemulsions loaded in chitosan and alginate-based microbeads. Int J Biol Macromol **140**: 682-696

Kemme M, Heinzel-Wieland R 2018: Quantitative assessment of antimicrobial activity of PLGA films loaded with 4-hexylresorcinol. J Funct Biomat **9**: 4

Kendall AC, Kiezel-Tsugunova M, Brownbridge LC, Harwood JL, Nicolaou A 2017: Lipid functions in skin: Di f erential e f ects of n-3 polyunsaturated fatty acids on cutaneous ceramides, in a human skin organ culture model. Biochim Biophys Acta (BBA) – Biomembranes **1859** (Part B):1679-1689

Komprda T 2012: Eicosapentaenoic and docosahexaenoic acids as in f ammation-modulating and lipid homeostasis in f uencing nutraceuticals: A review. J Funct Foods **4**: 25-38

Komprda T 2018: E f ect of n-3 long-chain polyunsaturated fatty acids on wound healing using animal models – a review. Acta Vet Brno **87**: 309-320

Komprda,T, Sladek Z, Sevcikova Z, Svehlova V, Wijacki J, Guran R, Do T, Lackova Z, Polanska H, Vrlikova L, Popelkova V, Michalek P, Zitka O, Buchtova M 2020: Comparison of dietary oils with di f erent polyunsaturated fatty acid n-3 and n-6 content in the rat model of cutaneous wound healing. Int J Mol Sci **21**: 7911

Liu E, Shao S, Li X, Meng X, Liu B 2021: Preparation, characterization of PLGA/chitosan nanoparticles as a delivery system for controlled release of DHA. Int J Biol Macromol **185**: 782-791

Meng FT, Ma GH, Qiu W, Su ZG 2003: W/O/W double emulsion technique using ethyl acetate as organic solvent: e f ects of its di f usion rate on the characteristics of microparticles. J Control Release **91**:407-416

Pettinelli N, Rodríguez-Llamazares S, Farrag,Y, Bouza R, Barral L, Feijoo-Bandín S, Lago F 2020: Poly(hydroxybutyrate-co-hydroxyvalerate) microparticles embedded in κ-carrageenan/locust bean gum hydrogel as a dual drug delivery carrier. Int J Biol Macromol **146**: 110-118

Rakotoarisoa, M, Angelov B, Garamus V, Angelova A 2019: Curcumin- and f sh oil-loaded spongosome and cubosome nanoparticles with neuroprotective potential against H_2O_2-induced oxidative stress in di f erentiated human SH-SY5Y cells. ACS Omega **4**: 3061-3073

Son G-H, Lee BJ, Cho C-W 2017: Mechanisms of drug release from advanced drug formulations such as polymeric-based drug-delivery systems and lipid nanoparticles. J Pharm Investig **47**: 287-296

Yang J, Ciftci ON 2020: *In vitro* bioaccessibility of f sh oil-loaded hollow solid lipid micro- and nanoparticles. Food Funct **11**: 8637-7647

A B

Fig. 1. Transmission electron microscopy of the representative samples of poly(lactic-co-glycolic) acid (PLGA)-
SRO\YLQ\O DOFRKRO 39$ QDQRSDUWLFOHV 13V HLWKHU HPSW\ $

Fig. 3. Inhibition activity of poly(lactic-co-glycolic) acid (PLGA)-polyvinyl alcohol (PVA) nanoparticles (NPs)
HLWKHU HPSW\ 3/*$ HPSW\ 39$ RU ZLWK HQWUDSSHG ¿VK RLO 3/*
DQG PHWKLFLOOLQ UHVLVWDQW 6 DXUHXV 056$ UHVSHFWLYHO\ C